SUPPLEMENTARY

The competition between dehydrogenation and dehydration reactions for primary and secondary alcohols over gallia: unravelling the effects of molecular and electronic structure via a two-pronged theoretical/experimental approach

Lorella Izzo[a], *Tommaso Tabanelli*[b], *Fabrizio Cavani*[b,c], *Paola Blair Vàsquez*[b], *Carlo Lucarelli*[d*], *Massimo Mella*[d*]

[a]Dipartimento di Biotecnologia e Scienze della Vita, Università degli Studi dell'Insubria, via J. H. Dunant 3, 21100 Varese (I)
[b]Dipartimento di Chimica Industriale "Toso Montanari", Università degli Studi di Bologna, Viale Risorgimento 4, 40136 Bologna (I)
[c]Consorzio INSTM, Research Unit of Bologna, Florence
[d]Dipartimento di Scienza ed Alta Tecnologia, Università degli Studi dell'Insubria, via Valleggio 11, 22100 Como (I)

Material characterization

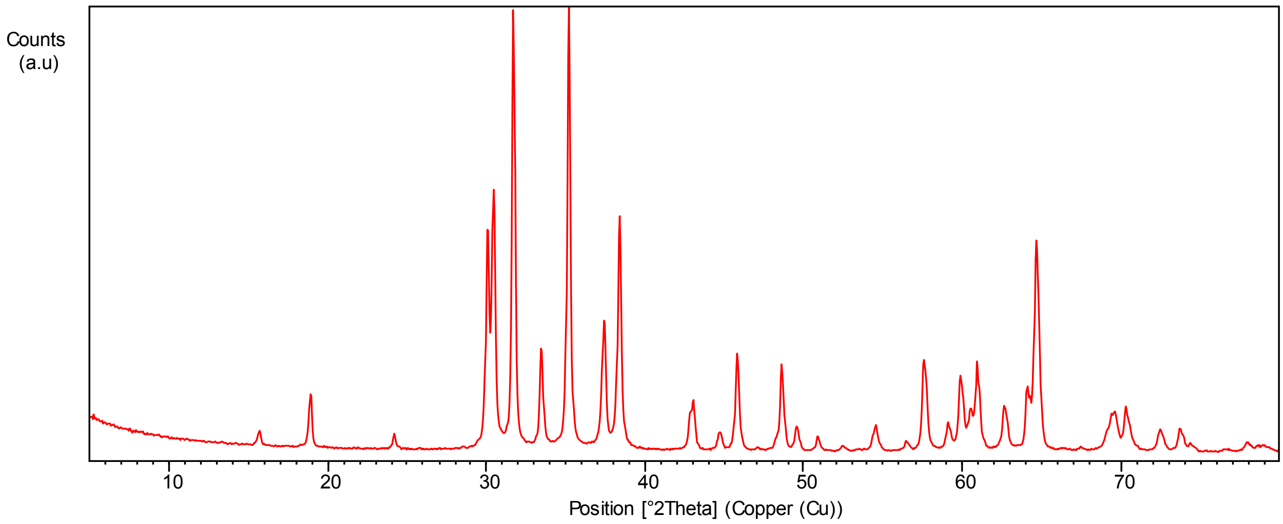

Figure S1: PXRD of commercial gallia; pure monoclinic phase (00-041-1103).

The catalyst has been further characterized by means of N_2 physisorption for the determination of the specific surface area (SSA) using the BET equation. The SSA of the commercial gallium oxide is equal to 7 m^2/g. Moreover, in order to have better insight on the acid and basic sites of the catalyst, both ammonia and carbon dioxide temperature programmed desorption (NH_3-TPD and CO_2-TPD respectively) have been performed on the fresh catalyst. The catalytic results are shown in Table S1 and in Figure S2.

µmol/g NH_3	µmol/m^2 NH_3	µmol/g CO_2	µmol/m^2 CO_2
43.7	6.2	21.8	3.1

Table S1: quantification of the acid and basic sites of the Ga_2O_3 catalyst.

Ga_2O_3 shows only weak basic sites on the catalyst surface; in fact, only a very small peak can be detected around 110°C during CO_2-TPD. On the other hand, NH_3-TPD shows the desorption of a considerable amount of ammonia in a wide range of temperature (from 130°C to 500°C) as reported in Figure S2. We take this as an indirect proof of the presence of different acid sites (from weak to medium strength). Moreover, both the erosion of the GaO-H stretching and the concomitant growth of the bands attributable to the dehydration products highlighted in the DRIFT experiments are clear indicators of the presence of Bronsted acid sites.

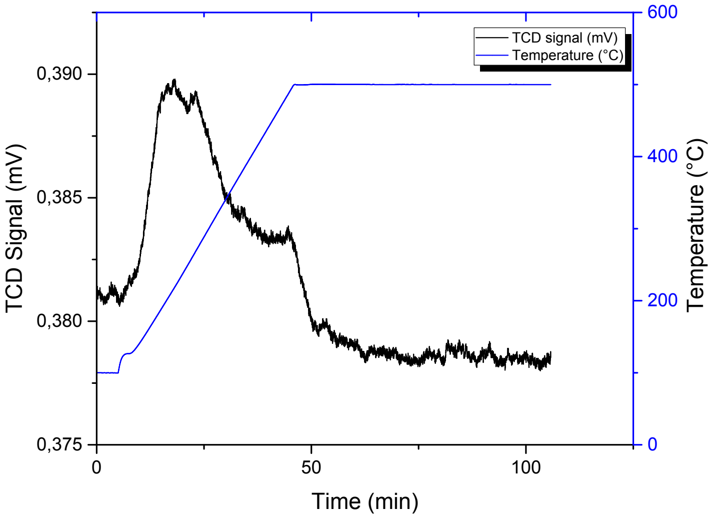

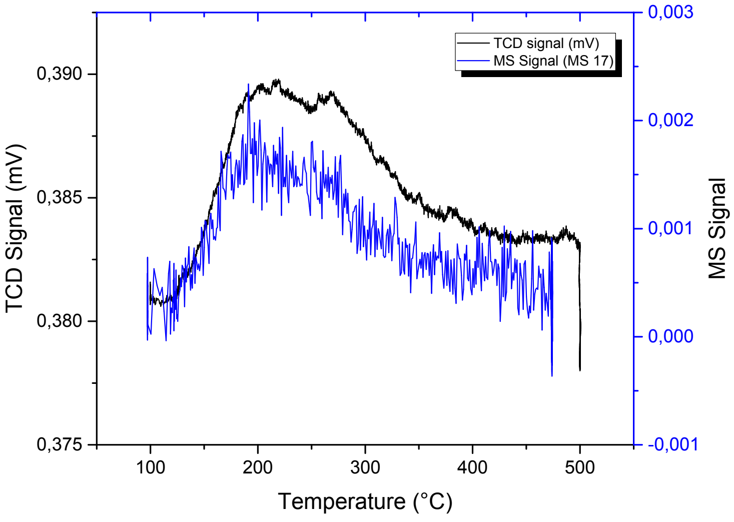

Figure S2: NH_3-TPD profiles for the Ga_2O_3

Regime testing for the studied processes

Thus, let us begin by pointing out that the presence of internal diffusional limitation can be safely assumed negligible given the specific surface area of the commercial gallia (7 m^2/g). We instead opted to run an additional dedicated experiment in order to understand whether or not we are in the presence of external diffusional limitation. Specifically, the reactor was loaded with half the amount (0.5g) of the catalytic material normally used and by halving the inlet flow rate to keep the contact time constant at the same reaction temperature; doubling the flow rate and catalyst mass was instead hampered by the presence of an excessive pressure drop. In these conditions, we analysed the transformation induced by the catalyst on ethanol, which was previously shown not to reach total conversion. The results in terms of alcohol conversion and product distribution (Figure S3) agree with the ones reported in the main text and obtained loading 1 g of Ga_2O_3. This proved that the reaction is under a kinetic regime and that the external diffusion is not limiting our reactions.

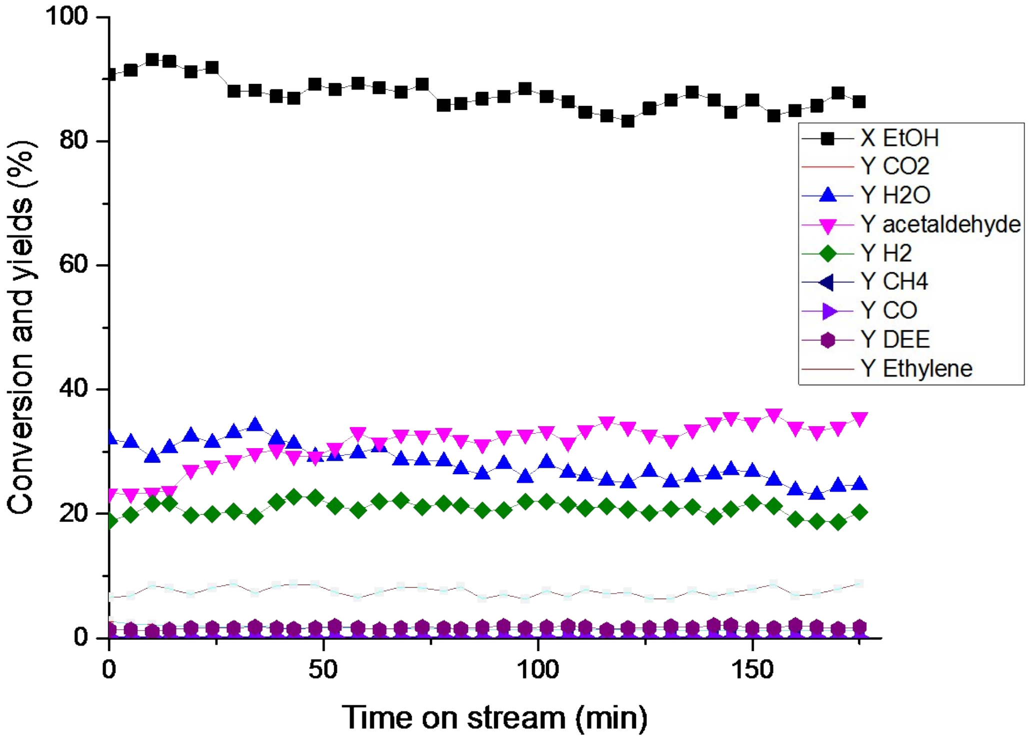

Figure S3: ethanol decomposition over Ga_2O_3 at 400°C, τ=1s, (molar feed composition benzyl alcohol:N_2=8:92). Catalyst loaded: 0.5g.

Table S2: Vibrational assignment (cm^{-1}) for 1-propanol over Ga_2O_3. The labels pre-deH_2 and post-deH_2O indicate the local minimum before the dehydrogenation TS, and the kinetic product of the dehydration (see Figure 1 for the reaction profile).

Description	**Wavenumber (cm^{-1})**						
	Calculated			**Experimental**			
	free	**Pre-deH_2**	**Post-deH_2O**	**free**	**Ads.**	**Des.**	**Flow**
ν OH free Ga_2O_3	**-**	**-**	**-**	***3658***	**-**	**-**	**-**
ν OH	3750	-	-	3320	-	-	-
ν GaO—H	-	-	3862	-	-	3458	3463
ν Ga-(O--H)-C	-	-	3837	-	3323	-	-
ν -CO—H--OGa	-	2984	-	-	-	3249	3264
ν_{as} CH_3 + ν_{as} CH_2 (propanal/propanoate)	-	-	3146	-	-	2984	2986
ν_s CH_3	3125	3130	-	2962	2966	-	2966
ν_{as} CH_3 + ν_{as} CH_2 (propanoate)	-	-	3112	-	-	2945	-
ν_{as} CH_2 + ν_{as} CH_3	3085	3114	-	2935	2939	-	2939
$\nu_{s\ of}$ CH_2 + ν_s CH_3	3047	3052	-	2925	2922	-	2918
ν_s CH_2 + ν CH (propanoate)	-	-	3094	-	-	2885	-
$\nu_{s\ if}$ CH_2 + ν_s CH_3 + ν OH	3040	3048	-	2875	2880	-	2880
ν_s CH_3 + ν_s CH_2 (propanal)	-	-	2998	-	-	-	2730
-	-	-	-	-	-	-	1759
ν -C—O--Ga (propanal)	-	-	1722	-	-	-	1733
(propanal)	-	-	-	-	-	1708	1701
ν C=C + δs CH_2 + δs CH_3 + δ CH (propylene)	-	-	1635	-	-	1648	1650
ν_{as} -COO--Ga (propanoate)	-	-	1509	-	-	1541	1540
δs CH_3 + δs CH_2 + δ CH (propanal)	-	-	1449	-	-	1472	1472
δs CH_3 + δs CH_2 + δ OH_{ip}	1502	1510	-	1456	1464	-	-
ν_s -COO--Ga (propanoate)	-	-	1430	-	-	1436	1430
δ OH_{ip} + ω CH_{2of} + δs CH_3	1420	1434	-	1382	1415	-	-
δ OH_{ip} + ω CH_{2if} + δs CH_3	1316	1401	-	1345	1389	-	1387
δ CH + δ CO + ω CH_2 + δs CH_3 + (propanal)	-	-	1407	-	-	-	1378
δ CH + ω CH_2 + δs CH_3 + (propanal)	-	-	1333	-	-	-	1339
τ CH_2 + τ CH_3 + δ CH (propanal)	-	-	1267	-	-	1301	1300
ω CC + ρ CH_3 + ω CH_2 (propanal)	-	-	1184	-	-	-	1258
τ CH_2 + τ CH_2 + δ OH_{ip}	1280	1309	-	1239	1340	-	-
ν CC + ω CH_2 + ρ CH_3 (propanal)	-	-	1031	-	-	-	1231-
τ CH_2 + ω CH_3 + δ OH_{op}	1143	1166	-	1097	1100	-	-
τ $CH_2(OH)$ + ω CH_2 + ν C-OH	1093	1138	-	1066	1069	-	1062
ρ CH_3 + ρ CH_2 + δ OH_{op} + ν CC	1054	1095	-	1056	1055	-	-
τ CH_3 + τ CH_2	939	1048	-	1016	1017	-	-
ν CC + δ OH_{op} + τ HOCO	898	998	-	966	971	-	-

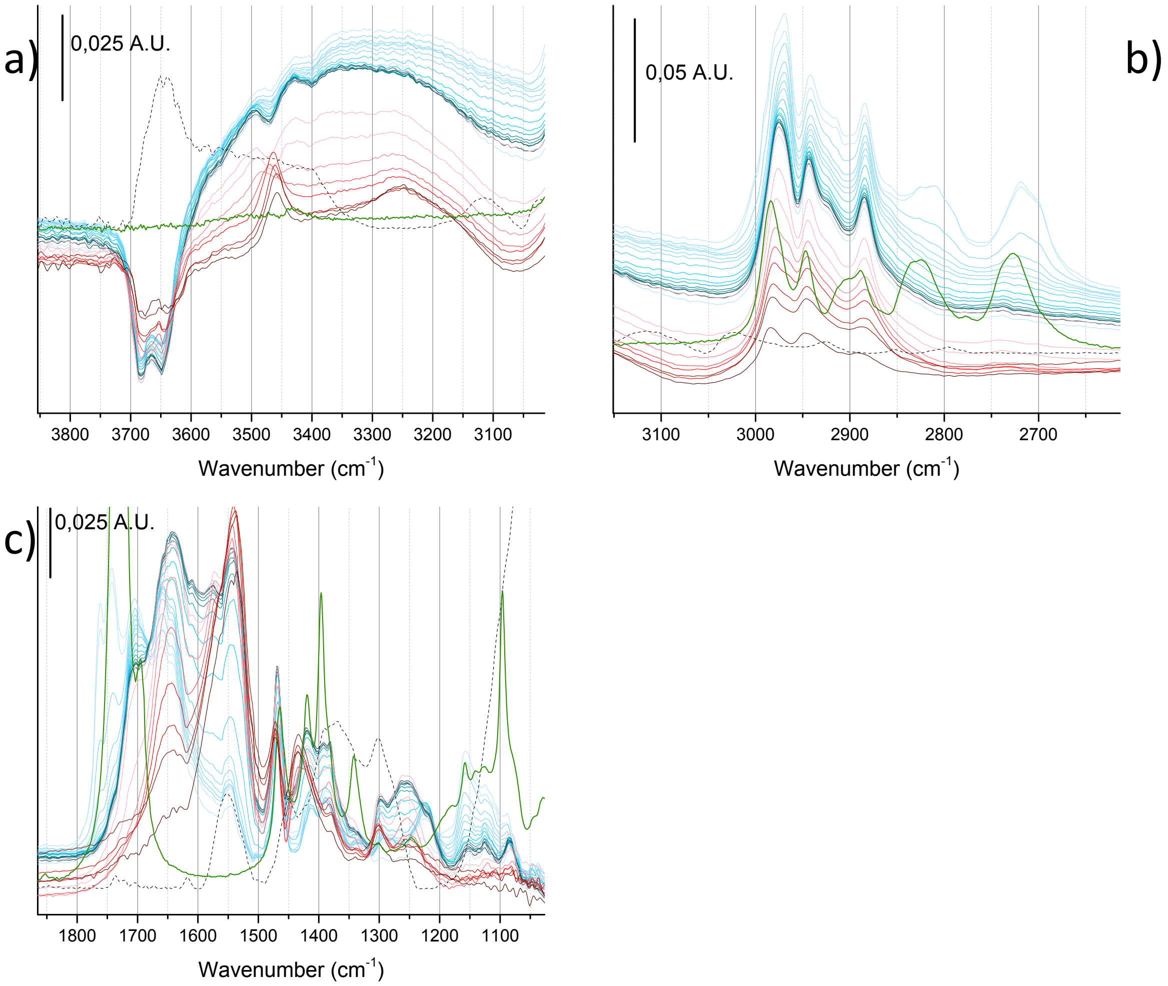

Figure S4: DRIFTS spectra of propionaldehyde over Ga_2O_3: a) between 3800 and 3100 cm^{-1}, b) between 3100 and 2600 cm^{-1} and c) between 1800 and 1000 cm^{-1} during propionaldehyde adsorption at 50°C (from azure to blue time elapsed after alcohol pulse); during propionaldehyde desorption (from pink to red spectra recorded each 50°C from 50°C to 450°C); line: green propionaldehyde, dotted pre-treated Ga_2O_3.

The propionaldehyde adsorption following the injection pulse produced a fast erosion of the band at 3658 cm^{-1} attributable to the OH stretching of surface chemisorbed water on Ga_2O_3 (Fig. S2 a). The intensity of all the bands increases reaching a maximum corresponding to duration of the pulse; it subsequently decreases reaching a steady state value. In the 3100 – 2600 cm^{-1} region (Fig. S2 b), it is possible to notice the presence of the bands at 2974, 2941, 2848, 2825, 2809, 2720 cm^{-1} attributable to the CH stretching modes of propanal shifted to lower wavenumber. In the 1800 – 1100 cm^{-1} region (Fig. S2 c) it is possible to observe a rapid erosion of the band relative to the C=O stretching (1701 cm^{-1}) with the concomitant growth of a series of bands at 1642, 1612, 1574, 1544. The disappearance of the band due to the C=O vibration confirm the weak interaction with the Ga_2O_3. Other bands are ascribable to the bending modes of the aldehyde. During desorption it is possible to notice the growth of the band at 3459 cm^{-1} attributable to the GaO-H stretching produced by the dehydration of propanal to produce propylene (Fig. S2 a). In the 1800 – 1100 region (Fig. S2 c) all the bands gradually disappear except the bands at 1574 and 1544 cm^{-1}, it is also noticeable the growth of a bands at 1430 cm^{-1}. These former bands could be attributed to the presence of propanoate specie adsorbed on the catalytic surface.

Table S3: Vibrational assignment (cm^{-1}) for 2-propanol over Ga$_2$O$_3$. The labels pre-deH$_2$ and post-deH$_2$O indicate the local minimum before the dehydrogenation TS, and the kinetic product of the dehydration (see Figure 1 for the reaction profile).

Description	**Wavenumber (cm^{-1})**						
	Calculated			**Experimental**			
	free	**Pre-deH$_2$**	**Post-deH$_2$O**	**free**	**Ads.**	**Des.**	**Flow**
ν OH free Ga$_2$O$_3$	**-**	**-**	**-**	***3658***	**-**	**-**	**-**
ν OH	3674	-	-	3340	3340	-	-
ν GaO—H	-	-	3856	-	-	3468	3453
ν -CO—H--OGa	-	3150/ 2700	3424	-	3232	3246	3252
ν_{as} CH$_2$ + ν CH (propylene)	-	-	3224	-	-	-	3102
- (propylene)-	-	-	-	-	-	-	3090
ν CH + ν_{as} CH$_2$ + ν_{as} CH$_3$ (propylene)	-	-	3160	-	-	-	3080
- (propylene)-	-	-	-	-	-	-	3071
ν_{as} CH$_2$ + ν CH (propylene)	-	-	3133	-	-	-	2989
ν_{as} CH$_3$ + ν CH (propylene)	-	-	3115	-	-	-	2980
$\nu_{as\ if}$ CH$_{3\ if}$ + ν -CO—H—Oga + ν CH	-	3145	-	-	-	-	-
ν -CO—H—Oga + $\nu_{as\ if}$ CH$_{3\ of}$ + ν CH	-	3141	-	-	-	-	-
ν -CO—H—Oga + $\nu_{as\ if}$ CH$_{3\ of}$ + ν CH	-	3133	-	-	-	-	-
$\nu_{as\ if}$ CH$_3$ + ν CH	3152	-	-	-	2979	2979	-
$\nu_{as\ if}$ CH$_3$ + ν CH	3145	-	-	2969	2971	2971	2969
$\nu_{as\ if}$ CH$_3$ + ν CH	3136	-	-	-	-	-	-
ν_{as} CH$_3$ (propylene)	-	-	3083	-	-	-	2952
$\nu_{as\ of}$ CH$_3$ + ν CH	3116	-	-	2931	2933	2933	2932
$\nu_{s\ if}$ CH$_3$ + ν CH	3050	3057	-	2917	2920	2920	-
- (propylene)-	-	-	-	-	-	-	2917
$\nu_{s\ if}$ CH$_3$ + ν CH	3032	3053	-	-	-	-	-
ν CH + $\nu_{as\ of}$ CH$_3$	3013	3040	-	2883	2887	2887	-
ν_s CH$_3$ (propylene)	-	-	3030	-	-	-	2889
ν CH	-	2091	-	-	2872	2872	-
- (propylene)-	-	-	-	-	-	-	2868
ν C=C + δs CH$_2$ + δ CH + δs CH$_3$ (propylene)	-	-	1688	-	-	-	1841
- (propylene)-	-	-	-	-	-	-	1821
ν CO + δs CH$_3$ (acetone)	-	-	1727	-	-	-	1738
ω CH$_3$ + δs CH$_2$ (propylene)	-	-	1497	-	-	-	1665
ω CH$_3$ + δs CH$_2$ (propylene)	-	-	1479	-	-	-	1649
δs CH$_2$ + δ CH + ω CH$_3$ (propylene)	-	-	1453	-	-	-	1636
ν_{as} C-O (hemiacetale)		--	-	-	-	1546	-
δs CH$_3$ + δ CH	1529	-	-	1466	1468	1468	-
τ CH$_3$ + τ CH$_3$ + δ_{op} CH + δ CC (propylene)	-	-	1424	-	-	-	1445
ν_s C-O (hemiacetale)	-	-	-	-	-	1423	-
δs CH$_3$ + δ CH + δ OH$_{ip}$	1515	1543	-	1407	1413	1413	-
δs_{if} CH3 + δ CH + ν CC + δ OH$_{ip}$	1443	1506	-	1378	1382	1382	-
δs_{if} CH3 + δ CH + ν CC + δ OH$_{ip}$	1428	1483	-	1369	1371	1371	1370
δs_{if} CH3 + ν CC (acetone)	-	-	1400	-	-	-	1354
ν CC + δ CH + ω CH$_3$	1368	1462	-	1340	1341	1341	-

δ OH_{ip} + ρ CH_3 + δ CH	1269	-	-	1308	-	1308	-
δ CH + δ CO-H--OGa + ω CH_3	-	1312	-	-	1252	1252	-
ν CC + δs CH_3(acetone bonded)	-	-	1284	-	-	-	1231
ν CC + δs CH_3(acetone free)	-	-	1250	-	-	-	1214
ν CC + δ OH + ω CH_3	1200	1283	-	1161	1164	1164	1163
δ CH + ω CH_3 + δ CC	1156	1214	-	1127	1132	1132	1130
δ OH_{ip} ν CC + ω CH_3	1092	1131	-	1108	-	-	-
ω CH_3 + δ OH + ν CC	947	1120	-	950	953	-	948
τ CH_3 + ν C-OH + δ CH	943	1022	-	816	-	-	-

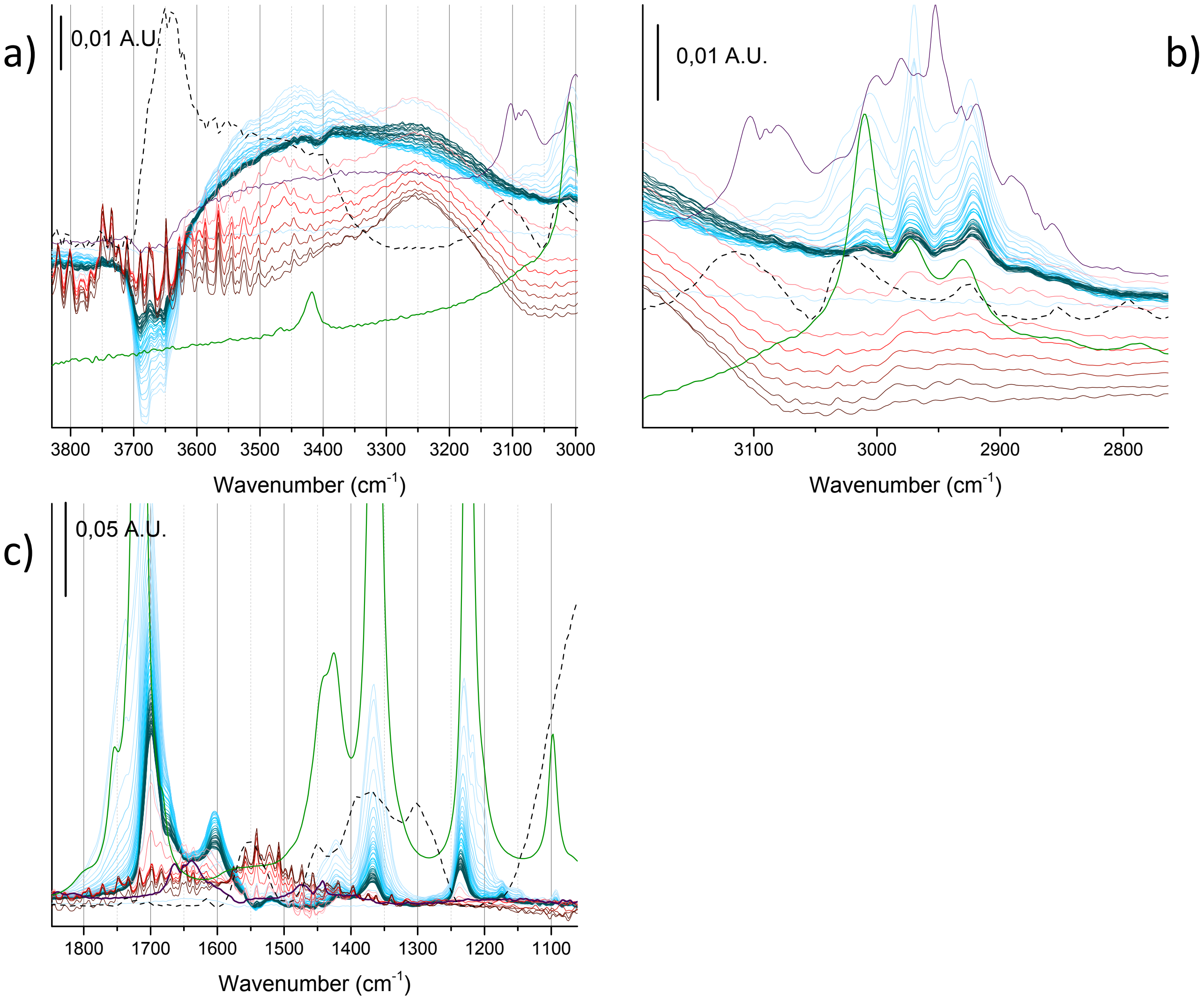

Figure S5: DRIFTS spectra of 2-propanone over Ga_2O_3: a) between 3800 and 3000 cm^{-1}, b) between 3000 and 2800 cm^{-1} and c) between 1800 and 1100 cm^{-1} during 2-propanone adsorption at 50°C (from azure to blue time elapsed after alcohol pulse); during 2-propanone desorption (from pink to red spectra recorded each 50°C from 50°C to 450°C); line: green 2-propanone, dotted pre-treated Ga_2O_3.

The acetone adsorption following the injection pulse produced a fast erosion of the band at 3658 cm^{-1} attributable to the OH stretching of surface chemisorbed water on Ga_2O_3 (Fig. S3 a). The intensity of all the bands increases reaching a maximum corresponding to duration of the pulse; it subsequently decreases reaching a steady state value. In all the spectral region (Fig. S3), it is possible to notice the presence of bands relative to the 2-propanone. Increasing temperature, during desorption, all the bands quickly disappear, evidencing the weak interaction of acetone with the catalytic surface. The growth of a pair of low intense and broad bands at 1544 and 1420 cm^{-1} attributable to the hemi-acetale specie was observed.

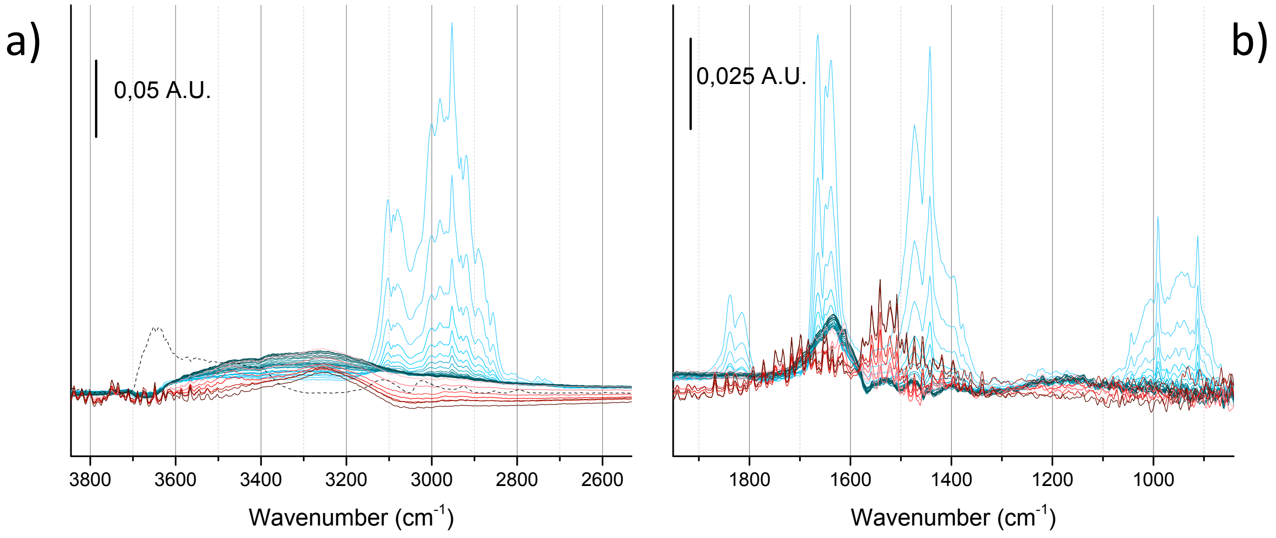

Figure S6: DRIFTS spectra of propylene over Ga_2O_3: a) between 3800 and 2600 cm^{-1} and b) between 1900 and 900 cm^{-1} during propylene adsorption at 50°C (from azure to blue time elapsed after alcohol pulse); during propylene desorption (from pink to red spectra recorded each 50°C from 50°C to 450°C); line: dotted pre-treated Ga_2O_3.

During the propylene adsorption, the intensity of all bands increases reaching a maximum corresponding to duration of the pulse; it subsequently decreases till completely disappearing.

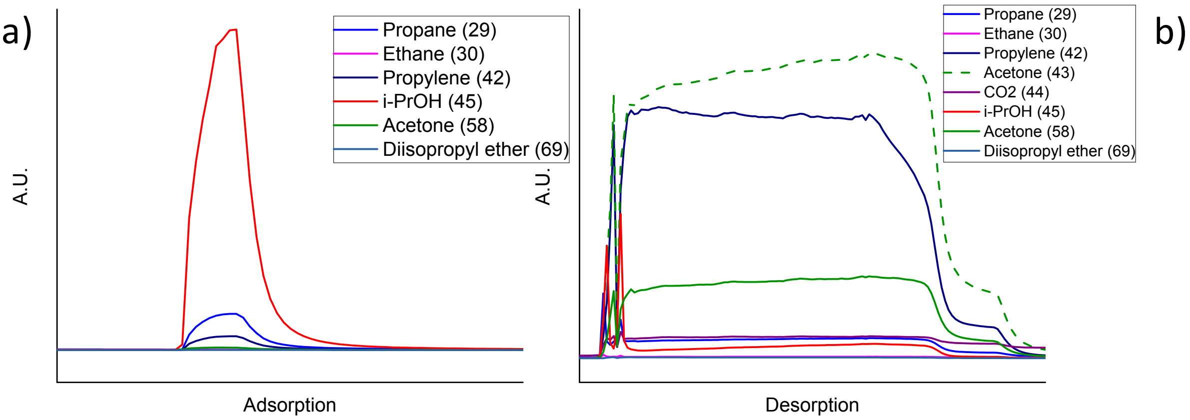

Figure S7: On-line MS-spectra recorded during the DRIFTS experiment feeding 2-propanol over gallia: a) pulse; b) desorption.

Table S4: relative energetic location of the kinetically relevant stationary points describing the dehydrogenation and dehydration pathways (in kcal/mol) of ethanol over alumina. The zero of the energy scale is set as the energy of the gas-phase alcohol and alumina cluster. Also, shown, there is the barrier difference (ΔΔE(TS)) between the TS's of the two reactive channels.

Alcohol	ΔΔE(TS) (E_{deH2O} - E_{deH2})	Dehydration		Dehydrogenation
		TS	ads	TS
ethanol	8.3	-12.7	-43.7	-4.3

Benzyl alcohol reactivity over gallia

The reactivity of an aromatic alcohol, for instance 1-phenyl ethanol, may be made non-trivial by the high melting point, which would have forced us to feed them as a solution with a suitable solvent. For this reason, tests were run with only benzyl alcohol (liquid at room temperature and boiling around 205°C) by feeding the liquid reagent in a nitrogen flow over Ga_2O_3 at 400°C in order to maintain similar conditions as the lighter aliphatic alcohols. In particular, a contact time of 1 second and a %vol of the alcohol of 8% was used for this test. The outlet gaseous stream from the reactor was condensed and recovered in 25 mL of acetonitrile and then analysed by means of a Thermo Focus off-line GC equipped with a FID detector and an Agilent HP-5 capillary column (temperature program: 50 °C for two min, then heating up to 280 °C at 10 °C min^{-1}, finally hold for five min). 20 µL of octane were added as internal standard for the quantification of the products. Benzyl alcohol and the main products were calibrated to obtain the corresponding response factor in the appropriate range of concentrations.

The catalytic results are shown in Figure S8.

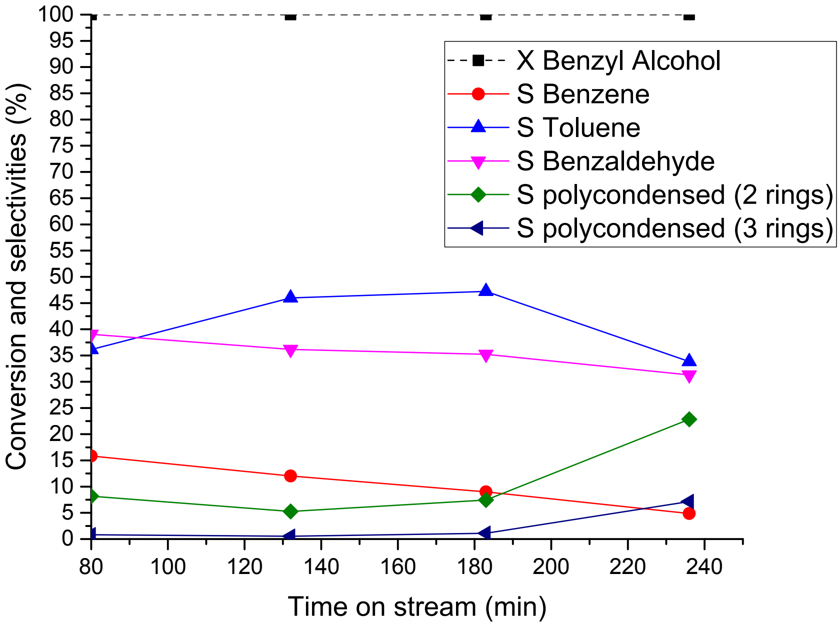

Figure S8: benzyl alcohol decomposition over Ga_2O_3 at 400°C, τ=1s, (molar feed composition benzyl alcohol:N_2=8:92). Selectivity are calculated as follow: $S_i=Y_i/\sum Y_i$.

Interestingly, a complete conversion of the fed benzyl alcohol has been achieved for more than 230 minutes of time on stream. As the dehydration reaction is prevented with this particular alcohol, the main detected products were benzaldehyde, toluene and benzene; a possible reaction pathway is proposed for these in Scheme S1. Noteworthy, a progressive increase of poly-condensated products can be witnessed by increasing the time on stream due to the parasitic benzylation and condensation reactions favored by the presence of acid sites on the catalyst. Moreover, the carbon balance of the reaction is always below 50% and progressively increase during the time on stream. This was attributed to the deposition of heavy carbonaceous residue not only over the catalyst surface (leading to a slow but progressive deactivation of the gallium oxide) but also over the reactor walls.

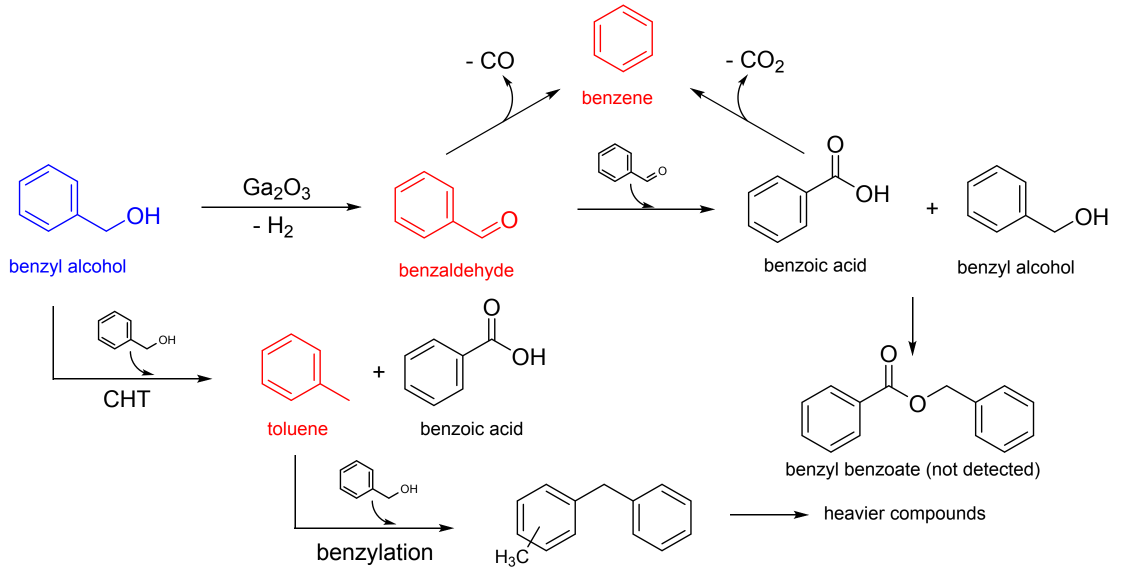

Scheme S1: proposed reaction pathway for the decomposition of benzyl alcohol over Ga_2O_3 at 400°C. The main products are highlighted in red.